Laboratory Investigation (2020) 100:250–264
https://doi.org/10.1038/s41374-019-0306-x

ARTICLE

Selective Ah receptor modulators attenuate NPC1L1-mediated cholesterol uptake through repression of SREBP-2 transcriptional activity

Gulsum E. Muku[1] · Ann Kusnadi[1] · Guray Kuzu[2] · Rachel Tanos[1] · Iain A. Murray[1] · Krishne Gowda[3] · Shantu Amin[3] · Gary H. Perdew[1]

Received: 25 April 2019 / Revised: 26 June 2019 / Accepted: 2 July 2019 / Published online: 15 August 2019

Abstract

The ability of the aryl hydrocarbon receptor (AHR) to alter hepatic expression of cholesterol synthesis genes in a DRE-independent manner in mice and humans has been reported. We have examined the influence of functionally distinct classes of AHR ligands on the levels of Niemann–Pick C1-like intracellular cholesterol transporter (NPC1L1) and enzymes involved in the cholesterol synthesis pathway. NPC1L1 is known to mediate the intestinal absorption of dietary cholesterol and is clinically targeted. AHR ligands were capable of attenuating cholesterol uptake through repression of NPC1L1 expression. Through mutagenesis experiments targeting the two DRE sequences present in the promoter region of the *NPC1L1* gene, we provide evidence that the repression does not require functional DRE sequences; while knockdown experiments demonstrated that this regulation is dependent on AHR and sterol-regulatory element-binding protein-2 (SREBP-2). Furthermore, upon ligand activation of AHR, the human intestinal Caco-2 cell line revealed coordinate repression of both mRNA and protein levels for a number of the cholesterol biosynthetic enzymes. Transcription of *NPC1L1* and genes of the cholesterol synthesis pathway is predominantly regulated by SREBP-2, especially after treatment with a statin. Immunoblot analyses revealed a significant decrease in transcriptionally active SREBP-2 levels upon ligand treatment, whereas the precursor form of SREBP-2 was modestly increased by AHR activation. Mechanistic insights indicate that AHR induces proteolytic degradation of mature SREBP-2 in a calcium-dependent manner, which correlates with the AHR ligand-mediated upregulation of the transient receptor potential cation channel subfamily V member 6 (*TRPV6*) gene encoding for a membrane calcium channel. These observations emphasize a role for AHR in the systemic homeostatic regulation of cholesterol synthesis and absorption, indicating the potential use of this receptor as a target for the treatment of hyperlipidosis-associated metabolic diseases.

Introduction

Coronary heart disease (CHD) is the leading cause of death worldwide with atherosclerosis being the major cause of initiation and progression of the disease [1]. Several processes regulate blood cholesterol levels, which include cholesterol de novo synthesis mainly in the liver and to a lesser extent in the intestine, dietary cholesterol absorption in the intestine, and biliary clearance and excretion. Dysregulation of any of these components is thought to be key to the development of hypercholesterolemia [2]. Statins are known to inhibit cholesterol biosynthesis by targeting the rate-limiting enzyme 3-hydroxy-3-methylglutaryl coenzyme A reductase (HMGCR) and have been shown to be very effective in reducing blood cholesterol, making them a standard therapy for the treatment of hypercholesterolemia

Supplementary information The online version of this article (https://doi.org/10.1038/s41374-019-0306-x) contains supplementary material, which is available to authorized users.

✉ Gary H. Perdew
ghp2@psu.edu

[1] Department of Veterinary and Biomedical Sciences, Center for Molecular Toxicology and Carcinogenesis, The Pennsylvania State University, University Park, PA 16802, USA

[2] Department of Biochemistry and Molecular Biology, Center for Eukaryotic Gene Regulation, The Pennsylvania State University, University Park, PA, USA

[3] Department of Pharmacology, Penn State College of Medicine, Hershey, PA 17033, USA

[3]. Another class of drugs has been developed to target the intestinal absorption of cholesterol in order to decrease its plasma levels [4]. The most commonly used drug in this class is ezetimibe (Zetia, Merck/Schering-Plough), capable of blocking both dietary and biliary cholesterol absorption [5]. Although the drug was developed and marketed in the absence of any known molecular target, later studies revealed its ability to specifically block Niemann–Pick C1-like intracellular cholesterol transporter (NPC1L1) [6]. This protein contains a sterol-sensing domain and is abundantly expressed in the small intestine and localized along the brush border in both human and mouse. In fact, targeted deletion of NPC1L1 in mice results in a drastic reduction of dietary cholesterol absorption [7]. However, unlike mice, the protein is also significantly expressed in the canalicular membrane of human hepatocytes, the site of bile acid secretion, where it is believed to play a role in the reabsorption of cholesterol into the liver [8]. Upon cholesterol loading in the intestine, NPC1L1 is transiently internalized through clathrin-coated vesicles to release the cholesterol at the cell interior. Ezetimibe has been shown to block the endocytosis of NPC1L1 induced by cholesterol loading [9]. In addition to mediating intestinal cholesterol uptake, a transgenic mouse model overexpressing NPC1L1 in the liver exhibited a dramatic decrease in biliary cholesterol concentration and an increase in plasma cholesterol levels, indicating a role of the protein in mediating biliary cholesterol reabsorption [10]. These observations suggest a key role for this protein in dietary and biliary cholesterol absorption both in the liver and the intestine.

The aryl hydrocarbon receptor (AHR) is a ligand activated basic-helix-loop-helix/Per-Arnt-Sim transcription factor that resides in the cytoplasm bound to heat shock protein 90, p23, and X-associated protein 2 [11]. Upon ligand binding, the complex undergoes a conformational transformation, which facilitates translocation to the nucleus, where AHR dimerizes with AHR nuclear translocator (ARNT). The AHR:ARNT heterodimer is capable of binding to dioxin-response elements (DRE) in the promoter of AHR target genes, such as cytochrome P-4501A1 (*CYP1A1)* and cytochrome P-4501B1(*CYP1B1*), to modulate gene expression. The AHR is activated by a wide array of chemicals but is best known as the receptor that mediates the toxicity of 2, 3, 7, and 8-tetrachorodibenzo-*p*-dioxin (TCDD). Rodents exposed to TCDD exhibit a myriad of effects such as wasting syndrome, altered lipid homeostasis, and impaired immune responses [12]. Genome-wide experiments examining the effect of TCDD on liver gene expression and promoter occupancy have revealed hundreds of genes either repressed or induced through the AHR [13, 14]. We have shown through the use of an AHR DNA-binding mutant that a number of genes are transcriptionally repressed by the AHR through a DRE-independent mechanism [15, 16]. There are three distinct classes of AHR ligands, namely agonists, antagonists, and selective ligands. Agonists induce the canonical AHR signaling pathway through binding of the AHR/ARNT heterodimer to dioxin responsive elements while antagonists repress such DRE-mediated responses. Selective AHR modulators (SAhRM) are defined as being capable of altering transcriptional activities, at least in part independent of DRE binding [17, 18].

The sterol regulatory element binding protein 2 (SREBP-2) is the predominant transcriptional regulator of enzymes involved in the cholesterol synthesis pathway. Sterol levels in cells, determined by either de novo synthesis or cellular cholesterol uptake, regulate the transcriptional activity of SREBPs. The precursor form of SREBP-2 resides in the endoplasmic reticulum membrane. When sterol levels are low, SREBP-2 cleavage-activating protein (SCAP) transports SREBP to the Golgi via vesicles. In the Golgi, SREBP-2 undergoes sequential proteolytic cleavage, and the transcriptionally active N-terminal of SREBP-2 is released and translocates to the nucleus. Mature SREBP-2 (mSREBP-2) is then capable of transcriptionally activating the genes that encode the enzymes involved in the cholesterol synthesis pathway. Conversely, under high intracellular sterol levels, precursor SREBP-2 (pSREBP-2) is retained in the endoplasmic reticulum membrane, and de novo cholesterol synthesis is diminished [19]. Lovastatin and other statins mediate their cholesterol-lowering activity through inhibition of HMGCR activity. However, lower levels of cholesterol lead to cleavage and activation of SREBP-2, which in turn increases expression of genes in the cholesterol synthesis pathway. This in effect is an autoregulatory mechanism that attempts to increase cholesterol production in the context of cholesterol lowering statin exposure.

Previously, we have identified the ability of the AHR to repress the hepatic expression of cholesterol synthesis genes in mice and humans [16]. NPC1L1 expression within both the liver and intestine has been shown to involve SREBP2 activity [20]. In this work we wanted to determine the AHR-mediated mechanism(s) that leads to repression of the expression of genes regulated by SREBP2. Interestingly, the use of the agonist TCDD or the selective ligands SGA360, and SGA315 reduced the levels of NPC1L1 coupled with attenuated expression of cholesterol synthesis genes and reduced cholesterol absorption in human Caco-2 cells, particularly after coadministration with lovastatin. This effect was shown to be regulated by SREBP-2. Furthermore, we investigated the mechanism behind the repressive effect of AHR and demonstrated that selective ligand activation leads to attenuation of mSREBP-2 protein levels and transcriptional activity. These results, in conjunction with our previous studies, clearly indicate a role for AHR in the regulation of cholesterol homeostasis.

Materials and methods

Reagents

Caco-2 cells were obtained from American Type Culture Collection (Manassas, VA). Lovastatin was obtained from A.G. Scientific (San Diego, CA). Cell viability assay was conducted using the CellTiter 96® NonRadioactive Cell Proliferation Assay (Promega, Madison, WI). pM vector was purchased from Clontech Laboratories, Inc. (Mountain View, CA). The reporter plasmid pFR-Luc was obtained from Agilent Technologies (La Jolla, CA). SGA360 and SGA315 were synthesized as previously described [17]. Primary antibodies used for immunoblot analysis are listed in Supplementary Table 1. [1,2-^{3}H(N)]-cholesterol was purchased from Perkin Elmer (Waltham, MA). Sodium taurocholate hydrate, 1-oleyl-rac-glycerol, and MG132 were obtained from Sigma-Aldrich (St. Louis, MO). β-Naphthoflavone (BNF) was purchased from Indofine Chemical Company (Hillsborough, NJ). BAPTA/AM and AEBSF were purchased from Cayman Chemicals (Ann Arbor, MI). Lovastatin was purchased from A.G. Scientific (San Diego, CA).

Cell culture

Caco-2 cells, a human epithelial colorectal adenocarcinoma cell line, were maintained in α-minimal essential medium (Sigma, St. Louis, MO), supplemented with 15% fetal bovine serum (HyClone Labs, Logan, UT), 100 U/mL penicillin, and 100 µg/mL streptomycin (Sigma) in a humidified incubator at 37 °C, with an atmospheric composition of 95% air and 5% CO_2. In treatment experiments cell culture medium contained 10% delipidated serum. Lipid was removed from serum by incubation with fumed silica powder (0.007 µm) as described by the manufacturer (Sigma, St. Louis, MO). Cells were exposed to Lovastatin (10 µM), BNF (10 µM), TCDD (10 nM), SGA360 (10 µM), SGA315 (10 µM), or carrier solution dimethyl sulfoxide for indicated time points. Enriched normal primary human hepatocytes were obtained through the Liver Tissue Cell Distribution System (University of Pittsburgh, PA). The isolated hepatocytes were seeded at ~90% confluence in 24-well collagen-coated dishes and cultured as previously described [20].

RNA isolation and reverse transcription

RNA samples were isolated from cell cultures using TRI reagent according to the manufacturer's instructions (Sigma-Aldrich). cDNA was generated using a high-capacity cDNA reverse transcription kit (Applied Biosystems™, Foster City, CA).

Real-time quantitative PCR

Real-time quantitative PCR was performed as previously described [20]. PerfeCTa™ SYBR® Green SuperMix for iQ (Quanta Biosciences, Gaithersburg, MD) was used and analysis was conducted using MyIQ software (Bio-Rad Laboratories, Hercules, CA). The PCR primers utilized are listed in Supplementary Table 2.

Gene silencing

AHR and SREBP-2 levels were decreased in Caco-2 cells using siRNA through electroporation as previously described [16], or Lipofectamine 3000 transfection reagent (Invitrogen, Carlsbad, CA) according to manufacturer's instructions. Seventy-two hours postelectroporation or transfection, RNA and protein samples were isolated.

Expression vector constructs

The hNPC1L1 promoter (−1741/+56)-pGL2 luciferase reporter vector and SRE mutant constructs were kindly provided by Waddah A. Alrefai (Univ. of Illinois) [21]. Primers were designed to incorporate a mutation in the two DRE core sequences (GCGTG) found in the proximal promoter of hNPC1L1. A QuikChange XL site-direct mutagenesis kit (Agilent Technologies, Cedar Creek, TX) and primers in Supplementary Table S2 were used to incorporate these mutations into pGL2-hNPC1L1-promoter vector. Luciferase activity was normalized to protein content.

Generation of stable reporter cell line

Caco-2 cells were transfected with pcDNA3 (Invitrogen) and pGL2-hNPC1L1-promoter vector at a ratio of 1/4 using Lipofectamine Plus essentially as described by the manufacturer. Clones were isolated after exposure to 400 µg/mL G418 for 10 days and screened for the ability of lovastatin to induce luciferase activity. Two clones were selected for further analysis.

GAL4-mammalian one hybrid assay

Transcriptionally active hSREBP-2 was subcloned from pcDNA3.1-2×FLAG-SREBP-2 into a pM vector. Caco-2 cells were seeded in 12-well plates 24 h before transfection. Cells were transfected with 20 ng of either pM vector or pM-hSREBP-2, along with their pFR-Luc target reporter plasmid (200 ng), and pSV-β-Gal vector (200 ng) using Lipofectamine 3000 reagent (Invitrogen, Carlsbad, CA) according to manufacturer's instructions. The luciferase activity of each sample was measured using a TD-20e

luminometer (Turner Systems, Sunnyvale, CA) using Luciferase Assay Substrate (Promega, Madison, WI) as suggested by the manufacturer. β-galactosidase activity was measured using a Thermo Scientific Pierce mammalian β-galactosidase assay kit [22].

Protein lysate preparation

Caco-2 cell extracts were prepared in MENG (25 mM MOPS, 2 mM EDTA, 0.02% sodium azide, and 10% glycerol), 1% Igepal CA-630 + protease inhibitor cocktail (Roche) + PhosSTOP phosphatase inhibitors (Roche, Indianapolis, IN). Cell homogenates were then centrifuged at 14,000 × *g* for 10 min and proteins were analyzed. For detection of SREBP-2, Caco-2 cells were lysed in RIPA buffer (10 mM Tris-HCl pH 8.0, 1 mM EDTA, 1 mM EGTA, 140 mM NaCl, 0.1% sodium deoxycholate, 0.1% sodium dodecyl sulfate (SDS), and 1% Igepal CA-630) + protease inhibitor cocktail + PhosSTOP phosphatase inhibitors. Lysates were cleared by centrifugation at 14,000 × g for 15 min and protein concentration was determined by Pierce™ BCA Protein Assay Kit (Thermo Fisher Scientific).

Immunoblot analysis

Caco-2 cell extracts were resolved on 8–10% SDS-tricine polyacrylamide gels. Proteins were transferred to PVDF membrane and detected using specific antibodies. Primary antibodies were visualized with biotin-conjugated secondary antibodies (Jackson Immunoresearch, West Grove, PA) and a subsequent incubation with ^{125}I-streptavidin followed by autoradiography. Quantification was performed with the ImageJ software. For immunoblot protein assessment of NPC1L1, SREBP-2, sterol regulatory element-binding protein cleavage (SCAP), and insulin-induced gene 1 (INSIG1), the Wes capillary system was utilized (Protein Simple, San Jose, CA). The Wes system was used with certain antibodies in order to minimize background.

Preparation of cholesterol micelle solution

Cholesterol micelles were prepared as described previously [23]. Briefly, 3 mM sodium taurocholate, 30 μM monoolein, 1 μM cholesterol, and 4 nM [1,2-^{3}H(N)]-cholesterol were mixed thoroughly by vortex in M199 media (Life Technologies, Carlsbad, CA) and kept in 37 °C for at least 2 h.

Cholesterol uptake assay

Caco-2 cells were cultured to complete confluency in six-well plates in α-MEM supplemented with 15% FBS and 1% penicillin/streptomycin. After 48 h treatment with SGA 360 (10 μM) or SGA315 (10 μM) in α-MEM containing 5% delipidated FBS and 1% penicillin/streptomycin, cells were washed twice with M199 media and incubated with M199 media containing cholesterol micelles for 30 min. Cells were then washed twice with cold PBS and lysed in 0.5 mL of 0.2 N NaOH. A total of 0.4 mL of the lysate was used to measure radioactivity by scintillation counter. The results were optimized to protein concentration and expressed as dpm/mg protein.

RNA-sequencing analysis

Total RNA was isolated and libraries were prepared from Caco-2 cells as previously described [22]. Briefly, RNA samples were poly-A selected and barcoded libraries were made from each sample using the Illumina TruSeq Stranded mRNA Library Prep Kit, according to the manufacturer's protocol. qPCR (Kapa kit) was then performed on all libraries to determine concentration. The equimolar pool of all barcoded libraries was sequenced on the Illumina HiSeq 2500 in Rapid Run mode using 100 nt single read sequencing at the the Pennsylvania State University Genomics Core Facility. RNA-seq reads were aligned to the Homo sapiens genome (hg19, RefSeq genes) using TopHat version 2.0.13 with default parameters [24]. Alignment results are given in Table S1. Reads mapping to genes were counted using HTseq-count version 0.5.4p3 with parameters "-s no -a 10 –nonunique all" [25]. Significance of expression change was calculated in the R programming environment (http://r-project.org) using the "limma" package. The GEO accession number is GSE130234.

Statistical analysis

All experiments were repeated between 2 and 4 times, and were performed with at least triplicate experimental samples for each treatment. Statistical results were essentially the same on each replicate experiment. Data were analyzed using one-way ANOVA (Tukey's test) in GraphPad Prism (v.6.01) software to determine statistical significance between treatments. P-values < 0.05 were considered statistically significant ($^{*}P < 0.05$; $^{**}P < 0.01$; $^{***}P < 0.001$; $^{****}P < 0.0001$). The "letter" without an asterisk is the reference data while the "letter" with an asterisk are being compared with the reference data.

Results

AHR attenuates NPC1L1 expression and cholesterol absorption in human cells

We chose to use the AHR ligands SGA360 and SGA315 for these studies. SGA360 fails to induce AHR translocation

into the nucleus or heterodimerization with ARNT [22]. While SGA315 exhibits partial agonist activity [17]. Lovastatin treatment effectively lowers cellular cholesterol levels leading to activation of SREBP-2. To determine the ability of AHR ligands to repress NPC1L1 levels induced by lovastatin, we used the intestinal human cell line Caco-2 cotreated with lovastatin and AHR ligands. Lovastatin led to a significant increase in NPC1L1, and selective ligands SGA360 and SGA315 attenuated lovastatin-induced NPC1L1 at both the mRNA and protein levels (Fig. 1a, b), whereas TCDD did not yield a statistically significant change. We also examined the effects of AHR ligands on hepatic *NPC1L1* expression in primary human hepatocytes. Similar to Caco-2 gene expression data, exposure of primary human hepatocytes to SGA360 or BNF led to a significant repression of *NPC1L1* mRNA levels, both basally and in response to lovastatin exposure (Fig. S1).

To demonstrate that attenuation of NPC1L1 expression is mediated by the AHR, we utilized siRNA to decrease the AHR levels in human Caco-2 cells. Reduction of AHR levels was associated with enhanced mRNA levels of *NPC1L1*, while SGA360 or SGA315 exhibited diminished efficacy in lowering *NPC1L1* transcripts in AHR-specific siRNA-transfected cells compared with control siRNA-transfected cells (Fig. 1c). AHR knockdown efficiency was validated by immunoblot analysis (Fig. S2). Consistent with reduced NPC1L1 expression upon AHR activation, SGA360 or SGA315 treatment significantly diminished cholesterol absorption by ~30% in Caco-2 cells, as evidenced by quantification of [^{3}H]-cholesterol levels in cell lysates (Fig. 1d).

Regulation of NPC1L1 expression by AHR is dependent on SREBP-2

To gain mechanistic insight into the AHR-mediated regulation of *NPC1L1* transcription, we established a human reporter Caco-2 stable cell line expressing luciferase under the control of the human *NPC1L1* promoter, which allows interpretation of the results to be restricted to

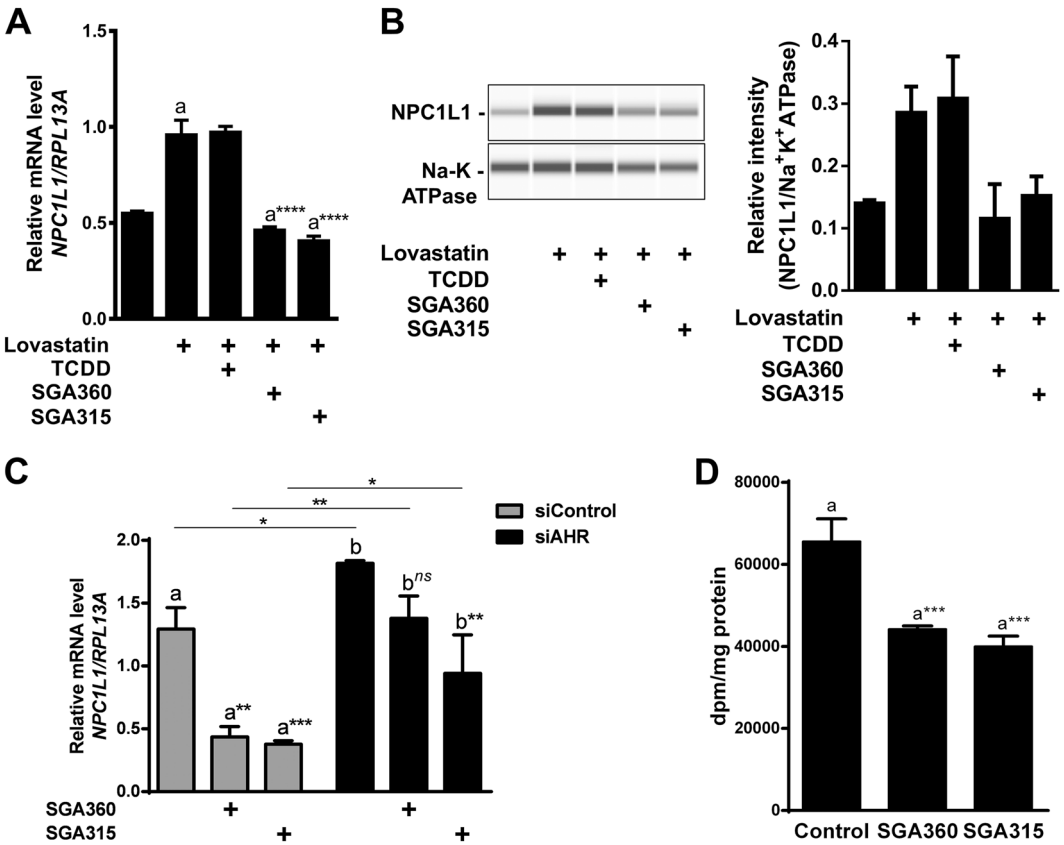

Fig. 1 AHR attenuates the expression of NPC1L1 and cellular cholesterol uptake. Caco-2 cells in the presence of 10% delipidated FBS were treated for 48 h with AHR ligands and lovastatin as indicated. NPC1L1 mRNA levels were assessed by qRT-PCR (**a**), and protein levels by WES (**b**). **c** Caco-2 cells were transfected with siRNA targeting AHR or control siRNA for 48 h, and then treated with ligands (10 μM) for an additional 24 h. NPC1L1 expression was assessed by qRT-PCR. **d** After 48 h of ligand treatment, Caco-2 cells were incubated with [1,2-^{3}H(N)]-cholesterol for 30 min and radioactivity was measured in the cell lysate. Data are presented as mean ± S.D., $n = 3$; significance was determined by one-way ANOVA (**a**, **b**, **d**) or two-way ANOVA (**c**), $^{**}p$-value ≤ 0.01, $^{***}p$-value ≤ 0.001 or $^{****}p$-value ≤ 0.0001

between −1741/+56 bp relative to the transcriptional start site. Two clones obtained after selection exhibited a dose-dependent increase in luciferase activity dependent on the concentration of lovastatin (Fig. 2a). Both clones yielded maximal luciferase activity at 10 μM lovastatin for 48 h. Clone 2 exhibited higher responsiveness to lovastatin compared with Clone 7, thus, Clone 2 was used in the subsequent study. Next, we determined the optimal time point for a maximal lovastatin response. The maximum NPC1L1-driven luciferase activity was achieved at 36 h in the presence of 10 μM lovastatin, and was maintained until the longest time point examined, 72 h (Fig. 2b).

Upon determination of exposure time and a dose of lovastatin, we then assessed the responsiveness of this stable cell line to SGA360 and TCDD. Lovastatin significantly increased NPC1L1-mediated luciferase activity (~sixfold), and SGA360 and TCDD repressed this lovastatin-induced luciferase activity, below control levels (Fig. 3a). SGA360 exhibited ~55% repression at 10 μM,

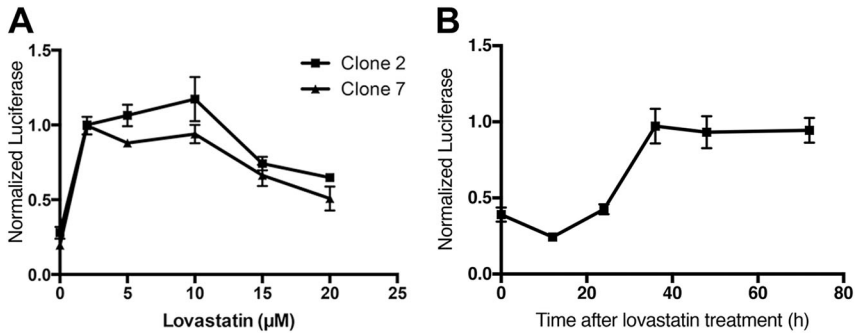

Fig. 2 Characterization of stable Caco-2 reporter cell line expressing *NPC1L1* promoter. **a** Dose-dependent effect of lovastatin on reporter activity in Clone 2 and Clone 7 after 48 h treatment. **b** Lovastatin (10 μM) mediated transcriptional activity was assessed over time in Clone 2

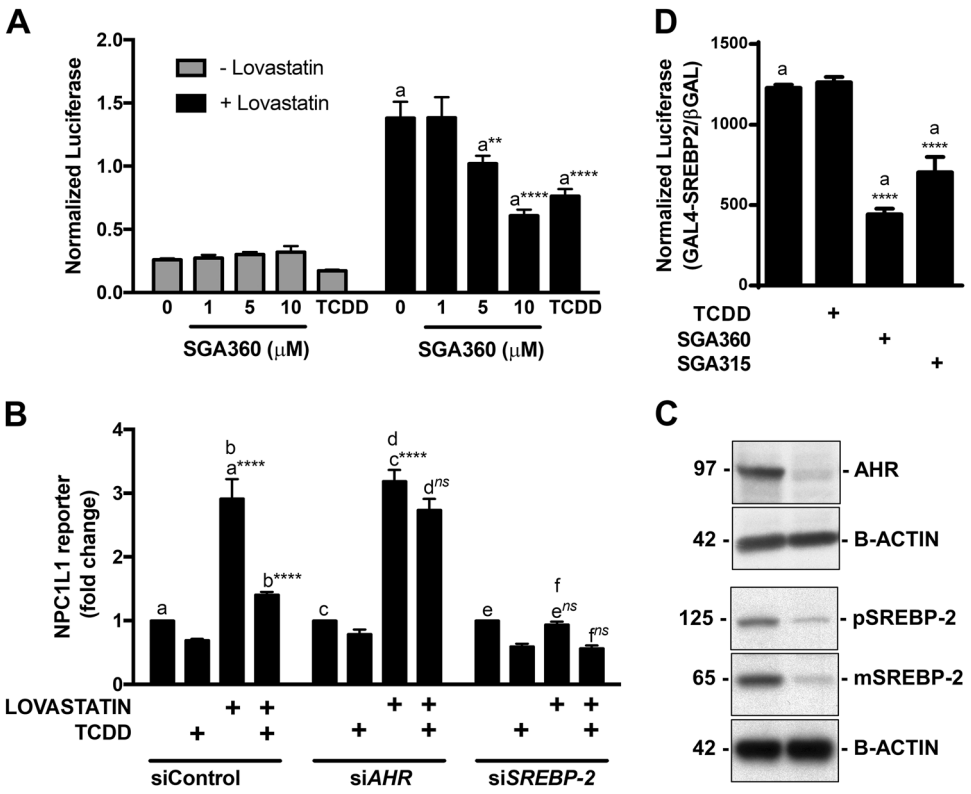

Fig. 3 Ligand activation of AHR represses NPC1L1-driven luciferase activity. **a** Stable Caco-2 reporter line was treated with lovastatin (10 μM), and TCDD (10 nM), SGA360 or SGA315 (10 μM) for 24 h, and luciferase activity was measured. **b** Stable Caco-2 reporter cells were transfected with siRNA targeting AHR, SREBP-2, or control siRNA by electroporation for 24 h, and then treated with lovastatin (10 μM) and TCDD (10 nM) for another 24 h. **c** Knockdown efficiency of AHR and SREBP-2 was validated by immunoblot analysis. The right-hand column depicts the specific siRNA knockdown samples. **d** Caco-2 cells were transfected with a GAL4-SREBP-2 construct by Lipofectamine 3000, and treated with ligands for 24 h. Data are presented as mean ± S.D., $n = 3$; significance was determined by one-way ANOVA (**d**), or two-way ANOVA (**a**, **b**), $^{**}p$-value ≤ 0.01, $^{***}p$-value ≤ 0.001 or $^{****}p$-value ≤ 0.0001

while TCDD displayed ~45% repression at 10 nM after 48 h cotreatment with lovastatin (Fig. 3a). In addition, AHR activation by the selective ligand SGA360, was able to significantly decrease the *NPC1L1* levels in a dose-dependent manner (Fig. 3a). To further confirm that this regulation is independent of DRE sequences in the human NPC1L1 promoter, we searched for core DRE sequences in the human *NPC1L1* gene promoter and found two putative core DRE sequences within 2000 bp from the transcriptional start site (Fig. S3A). Upon mutation of those two sites, SGA360 was still able to repress the lovastatin-induced *NPC1L1* reporter gene expression in transient transfections (Fig. S3B), indicating a DRE-independent mechanism through which the AHR suppresses *NPC1L1* expression.

To demonstrate the AHR-specificity of *NPC1L1* repression, stable Caco-2 cells were transfected with siRNA specific to *AHR*. Ligand treatment with TCDD failed to attenuate lovastatin-induced *NPC1L1* levels (Fig. 3b). Previous studies suggested that SREBP-2 transcriptionally regulates *NPC1L1* gene expression [21, 26]. Thus, we examined whether SREBP-2 is critical for AHR-mediated repression of *NPC1L1* expression. Upon siRNA knockdown of SREBP-2, lovastatin treatment failed to induce *NPC1L1*-driven luciferase, indicating the transcriptional response mediated by lovastatin is SREBP-2-specific. Diminished SREBP-2 levels also rendered the AHR ineffective in further lowering *NPC1L1* gene expression, suggesting the involvement of SREBP-2 in this regulation (Fig. 3b). AHR and SREBP-2 knockdown efficiency was validated by immunoblot analyses (Fig. 3c). To determine the effect of AHR ligands on SREBP-2 transcriptional activity, Caco-2 cells were transfected with the mature transcriptionally active form of SREBP-2 and a reporter plasmid construct. GAL4-SREBP-2 mammalian one hybrid assay demonstrated that SGA360 and SGA315 were able to attenuate SREBP-2-induced luciferase activity (Fig. 3d).

AHR attenuates the expression of cholesterol synthesis genes

Considering that intestinal epithelial cells play a critical role in cholesterol homeostasis, we wanted to examine the ability of SGA360 and SGA315 to alter the cholesterol biosynthesis pathway upon lovastatin treatment. We decided to focus on the ability of AHR ligands to attenuate lovastatin-induced expression of cholesterol biosynthetic genes due to the low basal expression level of these genes. Caco-2 cells were cotreated with lovastatin and SGA360 or SGA315 for 48 h in media containing delipidated serum, mRNA was isolated and sequenced. Based on the RNA-seq data, Gene Ontology analysis revealed that SGA360 and SGA315 significantly inhibited expression of a number of genes located in cholesterol and sterol biosynthetic processes, as well as regulation of these pathways (Fig. 4a–c). Several genes directly involved in the synthesis of cholesterol were found to be downregulated by AHR ligand treatment (Fig. 4d). On the other hand, the transcriptional regulator of these genes, encoded by the *SREBF2* gene, as well as the genes encoding for the factors involved in the proteolytic activation of SREBP-2, namely *SCAP*, site-1 protease, and site-2 protease did not exhibit a similar repression pattern upon ligand treatment. In addition, we determined that two direct AHR target genes, *CYP1A1* and *CYP1B1* were significantly repressed by SGA360 exposure and induced by SGA315 exposure (Fig. 4d). In contrast to SGA360, SGA315 has previously been shown to exhibit partial agonist activity [17].

We confirmed these findings by qRT-PCR analysis using Caco-2 cells cotreated with AHR ligands and lovastatin for 48 h. Ligand activation of AHR target gene *CYP1A1* revealed that the full agonist TCDD dramatically induced expression, while 10 µM SGA315 exhibited ~20% of the *CYP1A1* induction level observed with TCDD. In contrast, 10 µM SGA360 failed to induce *CYP1A1* (Fig. 5a). Eleven of the genes that comprise the cholesterol synthesis pathway were also examined by qRT-PCR and the results confirmed a significant level of repression by TCDD, SGA360, and SGA315. In particular, SGA360 and SGA315 exhibited a greater capacity toward repression compared with the agonist TCDD (Fig. 5a). Furthermore, SGA360 and SGA315 exhibited a dose-dependent repression of farnesyl-diphosphate farnesyltransferase (*FDFT1*), isopentenyl-diphosphate delta isomerase (*IDI1*), and mevalonate decarboxylase (*MVD*) genes after 24 h (Fig. 5b).

Similar to NPC1L1 data (Fig. 3b), siRNA knockdown of AHR resulted in an increase in constitutive mRNA levels of *HMGCR*, the rate-limiting enzyme of the cholesterol synthesis pathway. Significantly, the magnitude of transcriptional repression of *HMGCR* by SGA360 and SGA315 was attenuated when AHR levels were diminished, and there was a statistically significant decrease with *HMGCR* (Fig. 5c).

Next, we determined the ability of AHR ligands to alter the protein levels of enzymes in the cholesterol synthesis pathway in Caco-2 cells cotreated with lovastatin. Immunoblot analyses demonstrated that SGA360 and SGA315 mediated a statistically significant decrease in protein levels of the cholesterol synthesis enzymes examined, namely HMGCR, MVD, IDI1, farnesyl diphosphate synthase, FDFT1, and squalene monooxygenase (Fig. 6a). The repressive effect of AHR ligands on this pathway was not due to cytotoxicity in Caco-2 cells (Fig. S4).

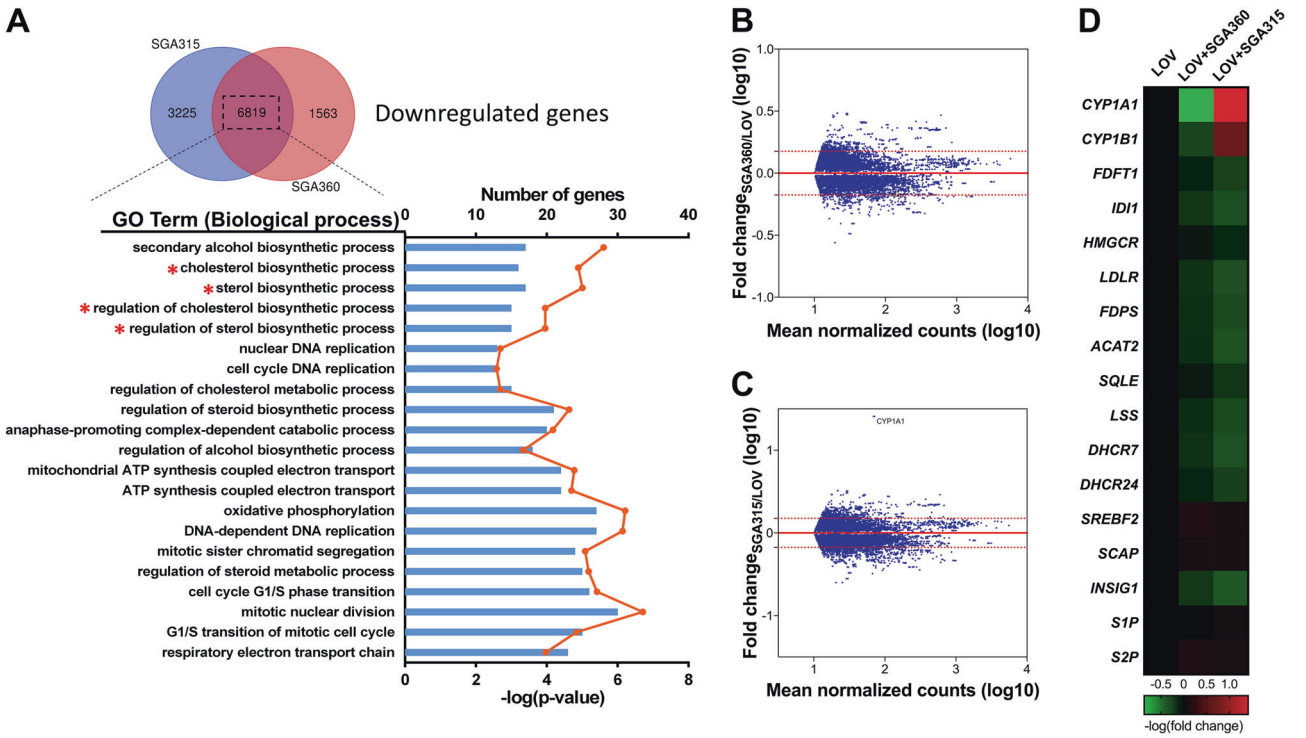

Fig. 4 RNA-sequencing identified a set of genes differentially expressed upon combination treatment with lovastatin and SGA360 or SGA315 in Caco-2 cells. Caco-2 cells were treated with lovastatin (10 μM) and SGA360 or SGA315 (10 μM) for 48 h and RNA isolated and sequenced. **a** Gene Ontology analysis revealed top canonical pathways altered upon SGA360 and SGA315 treatment in the presence of lovastatin. For a given pathway, blue bars indicate the number of downregulated genes, and the orange line indicates −log(*p*-value). The red asterisks denote pathways related to lipid biosynthesis. **b**, **c** MA plot representation of the gene expression data. The plots were obtained using Graphpad Prism, where M (*Y*-axis) represents the intensity ratio of [SGA360 + LOV] to [LOV] treatment, and **c** the intensity ratio of [SGA315 + LOV] to [LOV] treatment; fold change (log10), and A (*X*-axis) represents the average intensity of two treatment groups; mean normalized counts (log10). Red dashed lines represent the 1.5-fold change in gene expression. **d** Heatmap and histogram for a subset of genes involved in the cholesterol synthesis pathway that were down-regulated by SGA360 and SGA315. Each cell represents the fold change relative to the lovastatin treatment group (log10), for a given gene (row) in the specified treatment group (column). Cell colors indicate fold change level; red: upregulation, green: downregulation. All genes in this list have a significance greater than a p-value < 0.05

AHR attenuates transcriptionally active SREBP-2 levels by inducing proteolytic degradation of the mSREBP-2

To investigate the mechanism of AHR-mediated repression of cholesterol synthesis, we opted to examine the effect of AHR ligands on SREBP-2, the principal transcriptional regulator of genes in the cholesterol synthesis pathway. TCDD, SGA360, and SGA315 did not alter the mRNA levels of SREBP-2 in Caco-2 cells (Fig. 7a). However, selective ligands SGA360 and SGA315 significantly reduced the protein levels of the transcriptionally active mSREBP-2, while pSREBP-2 levels were modestly increased by ligand treatment in the presence of lovastatin (Fig. 7b, c). Interestingly, the expression of factors involved in SREBP-2 processing, namely SCAP and INSIG1 were not significantly altered at the protein level upon ligand treatment (Fig. S5).

This prompted us to examine the effect of AHR ligands on the half-life of mSREBP-2 protein levels. Cycloheximide administration led to a decrease in protein over time, as expected when protein synthesis is inhibited. However, the rate of protein turnover of the cleaved SREBP-2 was significantly enhanced in ligand treated samples compared with the control group (Fig. 8a). Addition of the protease inhibitor peptide MG132 significantly reversed the ratio of cleaved SREBP-2 to total SREBP-2 protein in ligand treated cells, whereas no change was observed in the control group (Fig. 8b). Similarly, serine inhibitor AEBSF reversed the AHR-mediated decrease in the mSREBP-2 protein levels to a greater extent than MG132 (Fig. 8c), indicating that SGA360 and SGA315 decrease the level of cleaved SREBP-2 protein at least partly through inducing proteolytic degradation.

Calcium chelation prevents AHR-mediated SREBP-2 inhibition

Calpains are calcium-dependent intracellular proteases. Thus, we opted to examine the involvement of calcium

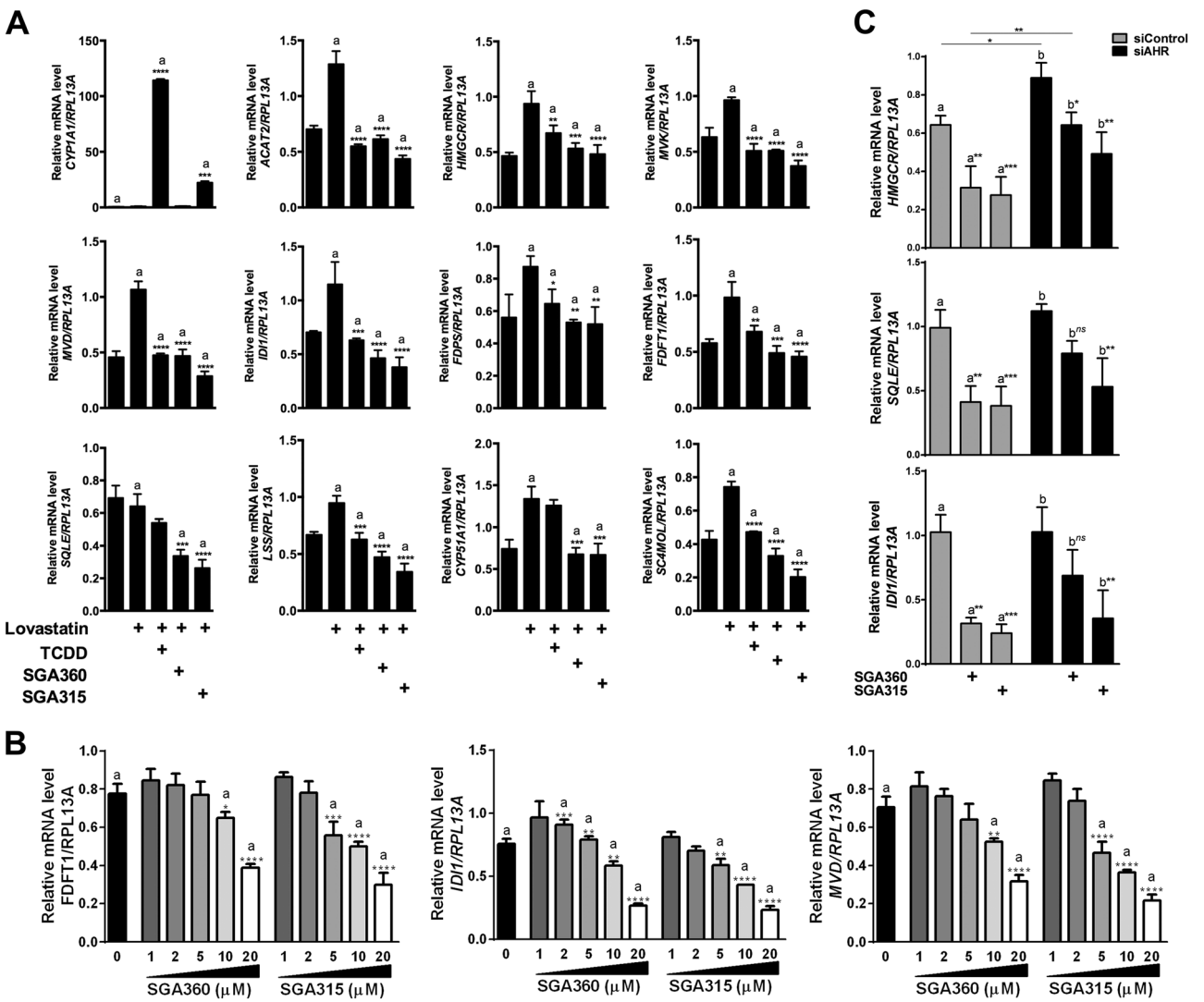

Fig. 5 AHR activation inhibits the expression of a number of genes directly involved in cholesterol synthesis. **a** Caco-2 cells were treated with lovastatin (10 μM) and TCDD (10 nM), SGA360, or SGA315 (10 μM) for 48 h or (**b**) at indicated doses for 24 h in the presence of delipidated FBS, and mRNA levels were determined by qRT-PCR. **c** Caco-2 cells were transfected with siRNA targeting AHR or control siRNA using Lipofectamine 3000 for 48 h, and then treated with ligands (10 μM) for another 48 h. RNA was isolated and expression levels of specific genes were determined. Data are presented as mean ± S.D., $n = 3$; significance was determined by one-way ANOVA (**a**) or two-way ANOVA (**b**, **c**) $^{**}p$-value ≤ 0.01, $^{***}p$-value ≤ 0.001 or $^{****}p$-value ≤ 0.0001

signaling in AHR-mediated repression of SREBP-2 activity. Cotreatment with the specific calcium chelator BAPTA/AM and selective AHR ligands SGA360 or SGA315 resulted in the loss of the repressive effect mediated by AHR ligands (Fig. 9a). However, BAPTA/AM alone led to a significant decrease in the basal level of the mSREBP-2, indicating a regulatory function of intracellular calcium in the level of mSREBP-2. Interestingly, RNA-seq analysis revealed that selective AHR activation led to a tenfold increase in the expression of transient receptor potential cation channel subfamily V member 6 (*TRPV6*) gene (Fig. 9c). A comparable increase in *TRPV6* transcripts was obtained by qRT-PCR analysis (Fig. 9d). Taken together, these results suggest a role for increased intracellular calcium flux through upregulation of *TRPV6* in AHR-mediated attenuation of SREBP-2 transcriptional activity.

Discussion

Currently, statins represent the mainstay of cholesterol-lowering drugs used to treat high blood cholesterol levels. Although they significantly reduce blood cholesterol levels and mortality associated with cardiovascular diseases, the optimal target levels for LDL in the blood are rarely attained in high-risk populations with a statin monotherapy. In addition, high-dose statins have been associated with serious side effects such as rhabdomyolysis and renal failure,

as well as drug–drug interactions [27]. Furthermore, the suppression of cholesterol synthesis by statin therapy is compensated for in part by a rise in intestinal cholesterol absorption [28]. Consistent with this concept, statin treatment was associated with an increase in the intestinal expression of NPC1L1 by 19% along with cholesterol synthesizing genes [29]. On the other hand, ezetimibe treatment blocks intestinal cholesterol absorption while reciprocally increasing synthesis [30]. Ezetimibe being the only cholesterol absorption inhibitor known to target NPC1L1 has shown a substantial interindividual variation in responsiveness to treatment. Although the mechanism is still not clear, variability might be partly accounted for by NPC1L1 polymorphisms [31]. In some patients, ezetimibe treatment dramatically decreased plasma cholesterol concentration, while in others it was barely effective, highlighting the need for the development of cholesterol uptake inhibitors [32].

Interestingly, the combination therapy targeting cholesterol synthesis and absorption by using statins and ezetimibe has already established a more pronounced decrease of LDL levels in the blood. Addition of ezetimibe to statin treatment resulted in a mean decrease in LDL of 25.8% ($n = 2020$) compared with 2.7% with statin alone ($n = 1010$) after 6 weeks ($p < 0.001$). Likewise, patients suffering from homozygous familial hypercholesterolemia showed a 14–21% additional decrease in their plasma LDL when ezetimibe was added to their statin regimen [33]. Zetia was also efficient in CHD patients with 71% of the patients attaining their LDL goal compared with 21% with statin alone [34]. In addition, ezetimibe treatment was proven to

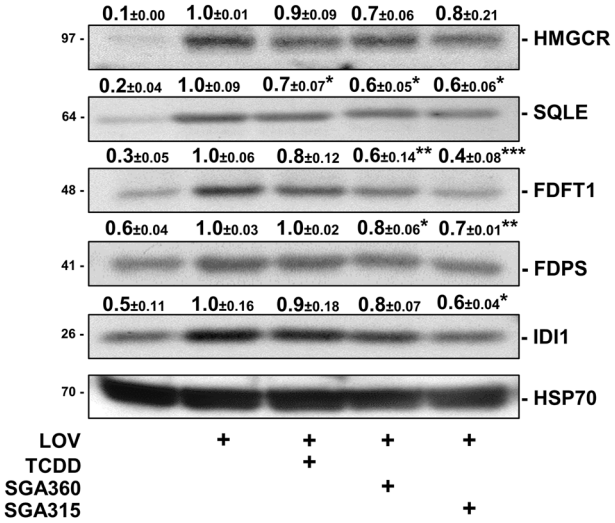

Fig. 6 AHR ligands are capable of diminishing the levels of cholesterol synthesis enzymes. Caco-2 cells were treated with lovastatin (10 μM) and TCDD (10 nM), SGA360, or SGA315 (10 μM) for 48 h in the presence of 10% delipidated FBS, and protein levels were assessed by immunoblot analysis. Data are presented as mean ± S.D., $n = 3$; significance was determined by one-way ANOVA, $^{**}p$-value ≤ 0.01, $^{***}p$-value ≤ 0.001 or $^{****}p$-value ≤ 0.0001

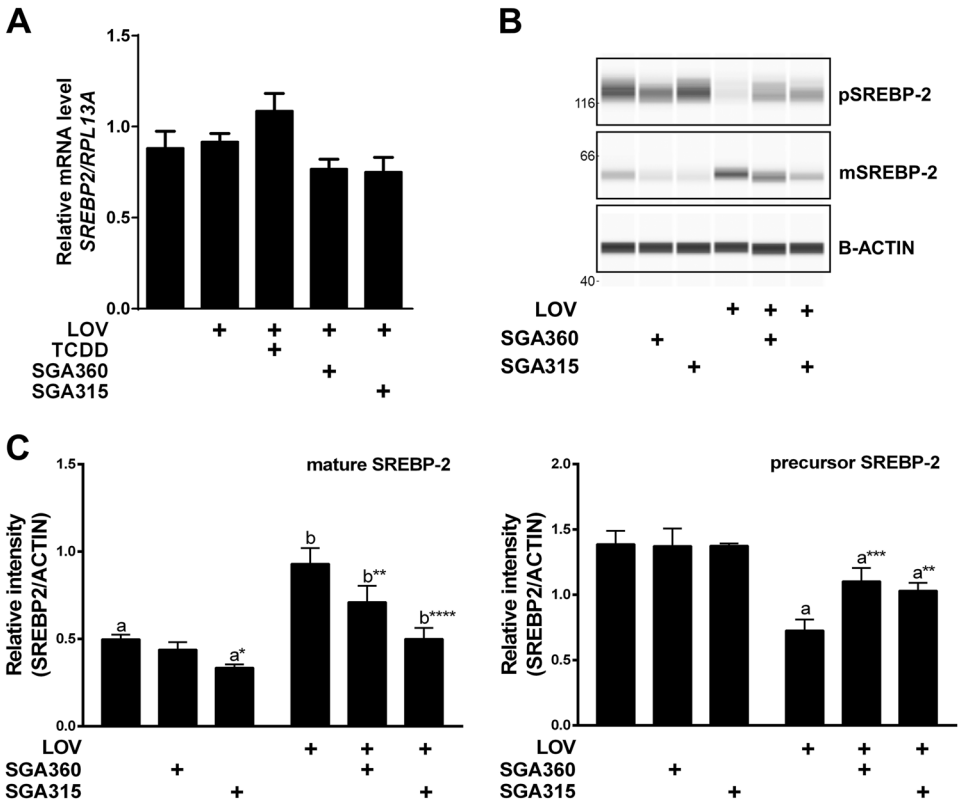

Fig. 7 AHR activation leads to a decrease in transcriptionally active SREBP-2 levels. After 48 h of treatment with lovastatin (10 μM) and AHR ligands (10 μM), SREBP-2 mRNA levels were examined by qRT-PCR analysis (**a**), and protein levels examined by WES analysis (**b**). **c** Data in panel B is quantified. p: precursor, m: mature. Data are presented as mean ± S.D., $n = 3$; significance was determined by one-way ANOVA, $^{**}p$-value ≤ 0.01, $^{***}p$-value ≤ 0.001 or $^{****}p$-value ≤ 0.0001

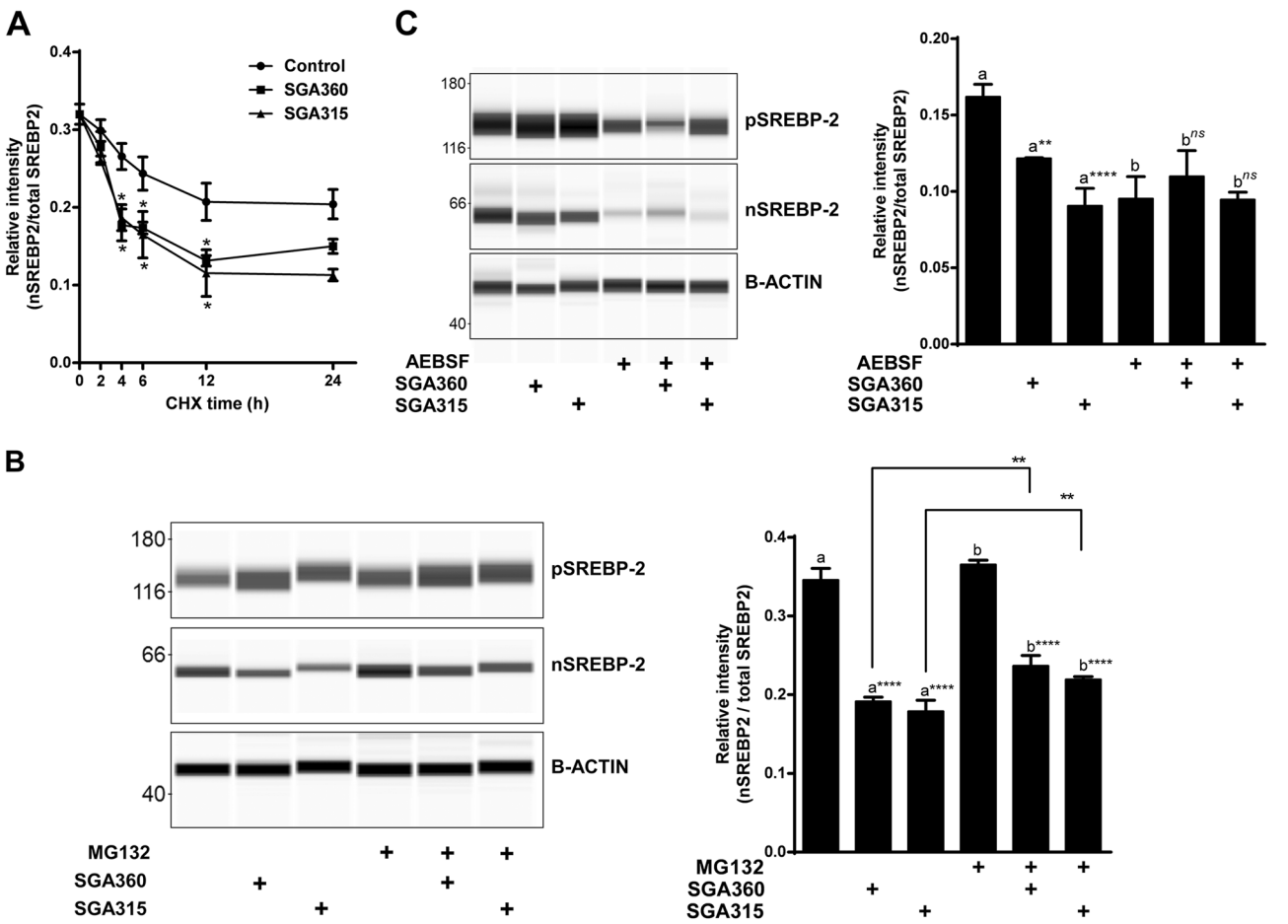

Fig. 8 AHR interferes with the stability of mSREBP-2. **a** Cyclohexamide (1 µg/mL) was administered to Caco-2 cells for the indicated time points, and SREBP-2 was examined by WES. Caco-2 cells were treated with SGA360 (10 µM) or SGA315 (10 µM), and MG132 (5 µM) (**b**) or AEBSF (10 µg/ml) (**c**) for 24 h in the absence of lovastatin, and SREBP-2 was examined by WES. p: precursor, m: mature. Data are presented as mean ± S.D., $n = 3$; significance was determined by one-way ANOVA, $^{**}p$-value ≤ 0.01, $^{***}p$-value ≤ 0.001 or $^{****}p$-value ≤ 0.0001

inhibit the development and progression of atherosclerosis in apolipoprotein E knockout mice [35]. Given the major effect of cholesterol absorption on plasma cholesterol levels as seen in patients using a combination treatment of statins and ezetimibe, finding new molecular targets for cholesterol absorption and synthesis is of great interest [36].

The involvement of AHR in cholesterol and lipid metabolism has been extensively described in rodents exposed to the high-affinity exogenous AHR ligand TCDD. Early studies demonstrated TCDD to reduce serum triglyceride levels, adipose tissue, and body weight. More recently, TCDD-mediated genome-wide AHR enrichment and differential gene expression analysis identified gene groups related to fatty acid and lipid metabolism in mice and rats [37, 38]. Oral administration of TCDD resulted in a ~25% decrease in total cholesterol in mouse serum [39]. Ligand activation of AHR has been demonstrated to induce spontaneous onset of hepatic steatosis in mouse models [40]. In addition, transgenic mice that express constitutively active hepatic AHR had increased accumulation of triglycerides in their liver [41]. Consistent with these findings, inhibition of AHR by its antagonists was demonstrated to be protective against Western diet-stimulated obesity and hepatic steatosis [42]. Similarly, AHR-deficient mice were found to be less susceptible to high-fat diet-induced obesity, liver steatosis, insulin resistance, and inflammation [43]. Furthermore, our laboratory has previously demonstrated that AHR activation attenuated the hepatic expression of genes involved in cholesterol and fatty acid synthesis in a DRE-independent manner [16, 44].

We examined here the ability of SAhRMs to influence mSREBP-2 proteins levels and transcriptional activity over a 48 h time frame in Caco2 cells. This long-term treatment conditions were necessary due to the time that it takes to reduce intracellular cholesterol levels leading to an increase level of mSREBP-2 levels. Under long-term treatment conditions TCDD induces rapid AHR translocation into the nucleus and dramatic downregulation of AHR levels through enhanced protein turnover. In contrast, SGA360

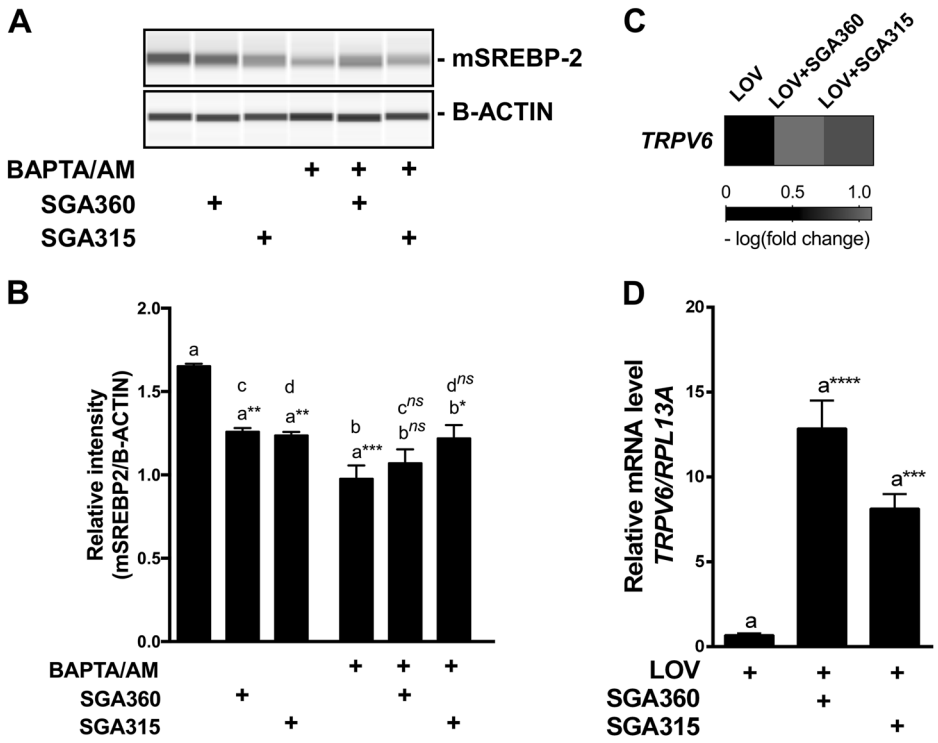

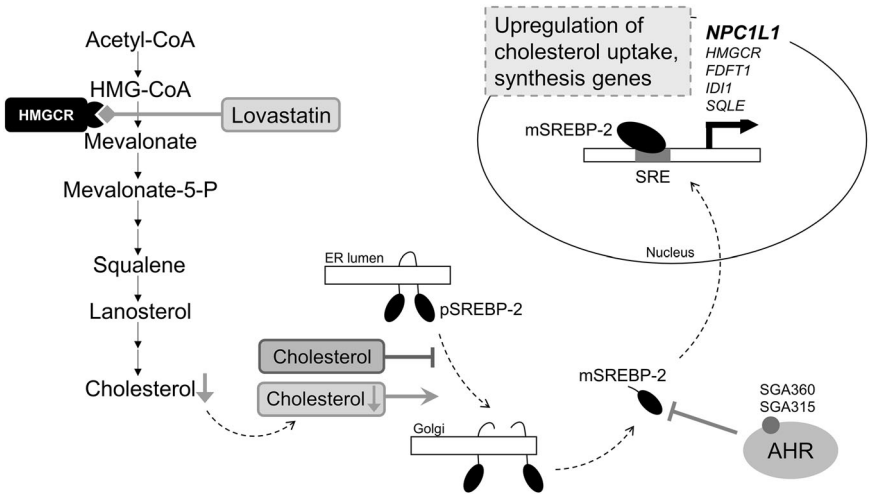

Fig. 9 Calcium chelation prevents AHR-mediated attenuation of SREBP-2. **a** BAPTA/AM (20 μM) was administered to Caco-2 cells in combination with carrier solvent, SGA360 (10 μM) or SGA315 (10 μM) for 24 h, and SREBP-2 protein level was assessed by WES. **c** Previous RNA-seq analysis described in Fig. 4 revealed altered expression of *TRPV6*. **d** Caco-2 cells were treated with lovastatin (10 μM) and SGA360 or SGA315 (10 μM) for 48 h and RNA isolated. *TRPV6* expression was validated by qRT-PCR. p: precursor, m: mature. Data are presented as mean ± S.D., $n = 3$; significance was determined by one-way ANOVA, $^{**}p$-value ≤ 0.01, $^{***}p$-value ≤ 0.001 or $^{****}p$-value ≤ 0.0001

Fig. 10 Proposed model of AHR-mediated inhibition of lovastatin-induced compensatory upregulation of cholesterol synthesis and uptake genes. Lovastatin inhibits the HMGCR enzyme, decreasing de novo cholesterol synthesis. However, a decrease in sterol levels leads to activation of SREBP-2 and subsequent upregulation of SREBP-2 target genes. Selective ligand-mediated modulation of the AHR attenuates this compensatory upregulation of NPC1L1 and cholesterol synthesis genes by diminishing the transcriptionally active mSREBP-2 protein levels

actually enhanced AHR levels after 24 h exposure. The precise mechanism of how SAhRM/AHR complex leads to mSREBP-2 turnover remains to be determined. However, we have previously shown that SGA360 actually causes cytoplasmic retention of the AHR [22]. Thus, suggesting that the AHR ligand-mediated decrease in mSREBP-2 levels likely occurs through protein–protein interaction events in the cytoplasm.

In this study, we described the involvement of the AHR in the regulation of NPC1L1 expression and demonstrated the ability of AHR agonist TCDD or the selective ligands SGA360 and SGA315 to attenuate the expression of cholesterol transporter NPC1L1, as well as cholesterol synthesis genes and subsequently decrease cholesterol uptake in human Caco-2 cells. Our data indicates that this regulation depends on SREBP-2, the principal transcriptional regulator

of cholesterol biosynthesis (Fig. 10). Furthermore, siRNA-mediated reduced AHR levels correlated with enhanced mRNA levels of *NPC1L1*. These results suggest a constitutive role for AHR in the regulation of NPC1L1 levels in the human intestine. Mechanistically, we demonstrated that SAhRM activation of AHR represses the expression of cholesterol synthesis genes by attenuating the levels of transcriptionally active mSREBP-2. The degree of AHR-mediated SREBP-2 inhibition appears to be significantly higher in the presence of lovastatin compared with the decrease in basal SREBP-2 levels upon AHR ligand exposure in the absence of lovastatin. AHR ligands, at least in part, induce the proteolytic degradation of the cleaved endogenous SREBP-2, and perhaps obstruct the processing of SREBP-2 without altering the expression of SCAP or INSIG1 protein. Previously reported E3 ubiquitin ligase activity of AHR might partly explain the observed decrease in the cleaved SREBP-2 levels [45, 46]. In the absence of lovastatin, selective AHR ligand elicit a moderate but statistically significant decrease in the basal level of cleaved SREBP-2, which was reversed by the inhibitor of calcium-activated calpains. Interestingly, we determined through RNA-seq analysis that AHR ligands markedly upregulated *TRPV6* gene expression, encoding for a membrane calcium channel protein, which is consistent with the previously reported increase in intracellular calcium by polycyclic aromatic hydrocarbons [47–50]. However, whether the increase in *TRPV6* expression observed here is a DRE-dependent or -independent mechanism will require further investigation. Upon chelation of calcium, AHR ligands were no longer able to repress the mSREBP-2 protein levels. It is plausible that elevated intracellular calcium activates calpains or other proteases, which then lead to proteolytic degradation of mSREBP-2 protein. However, calcium chelation alone decreased the basal expression of SREBP-2, suggesting that intracellular calcium might be involved in the regulation of SREBP-2 expression. Thus, AHR-induced repression of SREBP-2 transcriptional activity appears to be complex and likely involves the cross communication of multiple pathways. Nevertheless, future studies are needed to elucidate the main factor(s) involved in this process.

It is important to remember that the toxicity resulting from sustained AHR activation is mediated through DRE binding. Unlike the potent agonist TCDD, SGA360 exhibits no DRE-mediated activity. Thus, the ability of this compound to cooperatively attenuate the expression of cholesterol biosynthesis genes and subsequent cholesterol synthesis and absorption is likely in a DRE-independent manner pointing to the AHR as a potential therapeutic target in hypercholesterolemia. Our work provides the molecular basis for developing new cholesterol absorption drugs. The attenuation of SREBP-2 activity by selective activation of the AHR would overcome the compensatory upregulation of both cholesterol absorption and synthesis pathways, and thereby variability in the patient response to statin and ezetimibe treatments. Thus, the combination of statins or other cholesterol-lowering treatments such as a SAhRM holds considerable potential to further decrease total blood cholesterol. Whether these ligands exhibit the same efficiency in lowering cholesterol levels in vivo as observed in cell culture will require further investigation.

Acknowledgements We thank the Penn State Genomics Core Facility—University Park, PA, USA for RNA sequencing. We thank Curt Omiecinski and Denise Coslo for advice and technical assistance with the procurement and maintenance of primary human hepatocyte cultures from the Liver Tissue Cell Distribution System at the University of Pittsburgh, Pittsburg, PA, which is funded by National Institutes of Health Contract HHSN276201200017C. We also thank Marcia H Perdew for excellent editorial assistance. This work was supported in part by the National Institutes of Health Grants ES028244 and ES004869 and United States Department of Agriculture (Project 4607, GHP).

Compliance with ethical standards

Conflict of interest The authors declare that they have no conflict of interest.

References

1. Sanchis-Gomar F, Perez-Quilis C, Leischik R, Lucia A. Epidemiology of coronary heart disease and acute coronary syndrome. Ann Transl Med. 2016;4:256–256.
2. Trapani L, Segatto M, Pallottini V. Regulation and deregulation of cholesterol homeostasis: the liver as a metabolic 'power station'. World J Hepatol. 2012;4:184–90.
3. Stancu C, Sima A. Statins: mechanism of action and effects. J Cell Mol Med. 2001;5:378–87.
4. Clader JW, Burnett DA, Caplen MA, Domalski MS, Dugar S, Vaccaro W, et al. 2-azetidinone cholesterol absorption inhibitors: structure-activity relationships on the heterocyclic nucleus. J Med Chem. 1996;39:3684–93.
5. Hammersley D, Signy M. Ezetimibe: an update on its clinical usefulness in specific patient groups. Ther Adv Chronic Dis. 2017;8:4–11.
6. Garcia-Calvo M1, Lisnock J, Bull HG, Hawes BE, Burnett DA, Braun MP. The target of ezetimibe is Niemann-Pick C1-Like 1 (NPC1L1). Proc Natl Acad Sci USA. 2005;102:8132–7.
7. Altmann SW. Niemann–Pick C1 like 1 protein is critical for intestinal cholesterol absorption. Science. 2004;303:1201–4.
8. Chang TY, Chang C. Ezetimibe blocks internalization of the NPC1L1/cholesterol complex. Cell Metab. 2008;7:469–71.
9. Ge L, Wang J, Qi W, Miao H-H, Cao J, Qu Y-X, et al. The cholesterol absorption inhibitor ezetimibe acts by blocking the sterol-induced internalization of NPC1L1. Cell Metab. 2008;7:508–19.
10. Temel RE, Tang W, Ma Y, Rudel LL, Willingham MC, Ioannou YA, et al. Hepatic Niemann-Pick C1-like 1 regulates biliary cholesterol concentration and is a target of ezetimibe. J Clin Investig. 2007;117:1968–78.

11. Beischlag TV, Luis Morales J, Hollingshead BD, Perdew GH. The aryl hydrocarbon receptor complex and the control of gene expression. Crit Rev Eukaryot Gene Expr. 2008;18:207–50.
12. Birnbaum LS, Tuomisto J. Non-carcinogenic effects of TCDD in animals. Food Addit Contam. 2000;17:275–88.
13. Lo R, Celius T, Forgacs AL, Dere E, MacPherson L, Harper P, et al. Identification of aryl hydrocarbon receptor binding targets in mouse hepatic tissue treated with 2,3,7,8-tetrachlorodibenzo-p-dioxin. Toxicol Appl Pharmacol. 2011;257:38–47.
14. Sato S, Shirakawa H, Tomita S, Ohsaki Y, Haketa K, Tooi O, et al. Low-dose dioxins alter gene expression related to cholesterol biosynthesis, lipogenesis, and glucose metabolism through the aryl hydrocarbon receptor-mediated pathway in mouse liver. Toxicol Appl Pharmacol. 2008;229:10–9.
15. Patel RD, Murray IA, Flaveny CA, Kusnadi A, Perdew GH. Ah receptor represses acute-phase response gene expression without binding to its cognate response element. Lab Investig. 2009;89:695–707.
16. Tanos R, Patel RD, Murray IA, Smith PB, Patterson AD, Perdew GH. Aryl hydrocarbon receptor regulates the cholesterol biosynthetic pathway in a dioxin response element-independent manner. Hepatology. 2012;55:1994–2004.
17. Murray IA, Krishnegowda G, DiNatale BC, Flaveny C, Chiaro C, Lin J-M, et al. Development of a selective modulator of aryl hydrocarbon (Ah) receptor activity that exhibits anti-inflammatory properties. Chem Res Toxicol. 2010;23:955–66.
18. Murray IA, Flaveny CA, Chiaro CR, Sharma AK, Tanos RS, Schroeder JC, et al. Suppression of cytokine-mediated complement factor gene expression through selective activation of the Ah receptor with 3',4'-dimethoxy-alpha-naphthoflavone. Mol Pharmacol. 2011;79:508–19.
19. Brown MS, Goldstein JL. Cholesterol feedback: from Schoenheimer's bottle to Scap's MELADL. J Lipid Res. 2009;50: S15–S27.
20. Girer NG, Murray IA, Omiecinski CJ, Perdew GH. Hepatic aryl hydrocarbon receptor attenuates fibroblast growth factor 21 expression. J Biol Chem. 2106;291:15378–87.
21. Alrefai WA, Annaba F, Sarwar Z, Dwivedi A, Saksena S, Singla A, et al. Modulation of human Niemann-Pick C1-like 1 gene expression by sterol: role of sterol regulatory element binding protein 2. Am J Physiol Gastrointest Liver Physiol. 2007;292: G369–G376.
22. Muku GE, Lahoti TS, Murray IA, Podolsky MA, Smith KJ, Hubbard TD, et al. Ligand-mediated cytoplasmic retention of the Ah receptor inhibits macrophage-mediated acute inflammatory responses. Lab Investig. 2017;97:1471–87.
23. Feng D, Ohlsson L, Duan RD. Curcumin inhibits cholesterol uptake in Caco-2 cells by down-regulation of NPC1L1 expression. Lipids Health Dis. 2010;9:40.
24. Trapnell C, Pachter L, Salzberg SL. TopHat: discovering splice junctions with RNA-Seq. Bioinformatics. 2009;25:1105–11.
25. Anders S, Huber W. Differential expression analysis for sequence count data. Genome Biol. 2010;11:R106.
26. Pramfalk C, Jiang Z-Y, Cai Q, Hu H, Zhang S-D, Han T-Q, et al. HNF1alpha and SREBP2 are important regulators of NPC1L1 in human liver. J Lipid Res. 2010;51:1354–62.
27. Mansi I, Mortensen E. The controversy of a wider statin utilization: why? Expert Opin Drug Saf. 2013;12:327–37.
28. Miettinen TA, Gylling H. Cholesterol absorption efficiency and sterol metabolism in obesity. Atherosclerosis. 2000;153:241–8.
29. Tremblay AJ, Lamarche B, Lemelin V, Hoos L, Benjannet S, Seidah NG, et al. Atorvastatin increases intestinal expression of NPC1L1 in hyperlipidemic men. J Lipid Res. 2011;52:558–65.
30. Sudhop T, Lütjohann D, Kodal A, Igel M, Tribble DL, Shah S, et al. Inhibition of intestinal cholesterol absorption by ezetimibe in humans. Circulation. 2002;106:1943–8.
31. Hegele RA, Guy J, Ban MR, Wang J. NPC1L1 haplotype is associated with inter-individual variation in plasma low-density lipoprotein response to ezetimibe. Lipids Health Dis. 2005;4:16.
32. Pisciotta L, Fasano T, Bellocchio A, Bocchi L, Sallo R, Fresa R, et al. Effect of ezetimibe coadministered with statins in genotype-confirmed heterozygous FH patients. Atherosclerosis. 2007;194: e116–22.
33. Davis HR, Veltri EP. Zetia: inhibition of Niemann-Pick C1 Like 1 (NPC1L1) to reduce intestinal cholesterol absorption and treat hyperlipidemia. J Atheroscler Thromb. 2007;14:99–108.
34. Pearson T, Denke M, McBride P, Battisti WP, E. Brady W, Palmisano JE. Effectiveness of the addition of ezetimibe to ongoing statin therapy in modifying lipid profiles and attaining low-density lipoprotein cholesterol goals in older and elderly patients: Subanalyses of data from a randomized, double-blind, placebo-controlled. Am J Geriatr Pharmacother. 2005;3:218–28.
35. Davis HR, Compton DS, Hoos L, Tetzloff G. Ezetimibe, a potent cholesterol absorption inhibitor, inhibits the development of atherosclerosis in apoE knockout mice. Arterioscler Thromb Vasc Biol. 2001;21:2032–8.
36. Klett EL, Patel S. Genetic defenses against noncholesterol sterols. Curr Opin Lipidol. 2003;14:341–5.
37. Dere E, Lo R, Celius T, Matthews J, Zacharewski TR. Integration of genome-wide computation DRE search, AhR chIP-chip and gene expression analyses of TCDD-elicited responses in the mouse liver. BMC Genomics. 2011;12:365.
38. Nault R, Forgacs AL, Dere E, Zacharewski TR. Comparisons of differential gene expression elicited by TCDD, PCB126, βNF, or ICZ in mouse hepatoma Hepa1c1c7 cells and C57BL/6 mouse liver. Toxicol Lett. 2013;223:52–9.
39. Angrish MM, Dominici CY, Zacharewski TR. TCDD-elicited effects on liver, serum, and adipose lipid composition in C57BL/6 mice. Toxicol Sci. 2013;131:108–15.
40. Yao L, Wang C, Zhang X, Peng L, Liu W, Zhang X, et al. Hyperhomocysteinemia activates the aryl hydrocarbon receptor/CD36 pathway to promote hepatic steatosis in mice. Hepatology. 2016;64:92–105.
41. Lee JH, Wada T, Febbraio M, He J, Matsubara T, Lee MJ, et al. A novel role for the dioxin receptor in fatty acid metabolism and hepatic steatosis. Gastroenterology. 2010;139:653–63.
42. Moyer BJ, Rojas IY, Kerley-Hamilton JS, Hazlett HF, Nemani KV, Trask HW, et al. Inhibition of the aryl hydrocarbon receptor prevents Western diet-induced obesity. Model for AHR activation by kynurenine via oxidized-LDL, TLR2/4, TGFβ, and IDO1. Toxicol Appl Pharmacol. 2016;300:13–24.
43. Xu CX, Wang C, Zhang ZM, Jaeger CD, Krager SL, Bottum KM, et al. A aryl hydrocarbon receptor deficiency protects mice from diet-induced adiposity and metabolic disorders through increased energy expenditure. Int J Obes. 2015;39:1300–9.
44. Tanos R, Murray IA, Smith PB, Patterson A, Perdew GH. Role of the Ah receptor in homeostatic control of fatty acid synthesis in the liver. Toxicol Sci. 2012;129:372–9.
45. Ohtake F, Baba A, Takada I, Okada M, Iwasaki K, Miki H, et al. Dioxin receptor is a ligand-dependent E3 ubiquitin ligase. Nature. 2007;446:562–6.
46. Ohtake F, Fujii-Kuriyama Y, Kato S. AhR acts as an E3 ubiquitin ligase to modulate steroid receptor functions. Biochem Pharmacol. 2009;77:474–84.
47. Mounho BJ, Davila DR, Burchiel SW. Characterization of intracellular calcium responses produced by polycyclic aromatic hydrocarbons in surface marker-defined human peripheral blood mononuclear cells. Toxicol Appl Pharmacol. 1997;145:323–30.
48. Tannheimer SL, Barton SL, Introduction S, Ethier P, Burchiel SW. Carcinogenic polycyclic aromatic hydrocarbons increase intracellular Ca 2 and cell proliferation in primary human mammary epithelial cells. Carcinogenesis. 1997;18:1172–82.

49. Mayati A, Levoin N, Paris H, N'Diaye M, Courtois A, Uriac P, et al. Induction of intracellular calcium concentration by environmental benzo(a)pyrene involves a β2-adrenergic receptor/adenylyl cyclase/Epac-1/inositol 1,4,5-trisphosphate pathway in endothelial cells. J Biol Chem. 2012;287:4041–52.

50. N'Diaye M, Le Ferrec E, Lagadic-Gossmann D, Corre S, Gilot D, Lecureur V, et al. Aryl hydrocarbon receptor- and calcium-dependent induction of the chemokine CCL1 by the environmental contaminant benzo[*a*]pyrene. J Biol Chem. 2006; 281:19906–15.